JACS
JOURNAL OF THE AMERICAN CHEMICAL SOCIETY
COMMUNICATION
pubs.acs.org/JACS

Zinc Chelation with Hydroxamate in Histone Deacetylases Modulated by Water Access to the Linker Binding Channel

Ruibo Wu,[†,‡] Zhenyu Lu,[‡] Zexing Cao,[*,†] and Yingkai Zhang[*,‡]

[†]Department of Chemistry and State Key Laboratory of Physical Chemistry of Solid Surfaces, Xiamen University, Xiamen 361005, China
[‡]Department of Chemistry, New York University, New York, New York 10003, United States

Supporting Information

ABSTRACT: It is of significant biological interest and medical importance to develop class- and isoform-selective histone deacetylase (HDAC) modulators. The impact of the linker component on HDAC inhibition specificity has been revealed but is not understood. Using Born−Oppenheimer ab initio QM/MM MD simulations, a state-of-the-art approach to simulating metallo-enzymes, we have found that the hydroxamic acid remains to be protonated upon its binding to HDAC8, and thus disproved the mechanistic hypothesis that the distinct zinc−hydroxamate chelation modes between two HDAC subclasses come from different protonation states of the hydroxamic acid. Instead, our simulations suggest a novel mechanism in which the chelation mode of hydroxamate with the zinc ion in HDACs is modulated by water access to the linker binding channel. This new insight into the interplay between the linker binding and the zinc chelation emphasizes its importance and gives guidance regarding linker design for the development of new class-IIa-specific HDAC inhibitors.

Histone deacetylase enzymes (HDACs), which are responsible for the removal of acetyl groups from acetyl-lysine residues of histones and other cellular proteins, are central to the regulation of many vital cellular functions.[1−3] Inhibition of HDACs has emerged as a highly promising strategy for the development of new therapeutics against cancer and other human disorders.[4−8] A key challenge in HDAC inhibitor design is to control the class- and isoform-selective inhibition.[9−13] Most HDAC inhibitors, including two recent FDA-approved anticancer drugs, SAHA (suberoylanilide hydroxamic acid) and FK228, can be described by the cap−linker−chelator model.[14] As illustrated in Figure 1a, the chelator refers to the zinc binding group, the linker part mimics the aliphatic part of the acetyl-lysine side chain spanning the binding channel, and the cap component interacts with the rim region of the active site cavity. Recently, a novel chemical phylogenetic analysis[9] indicated the linker−chelator motif as the principal component to cluster HDAC inhibitors and revealed the impact of the linker component on HDAC inhibition selectivity, particularly for class-IIa HDAC enzymes. However, no mechanism has been suggested regarding the interplay between the linker binding and the zinc chelation.

Of 11 known isoforms of zinc-dependent HDACs in humans, structures of three HDAC isoforms in complex with

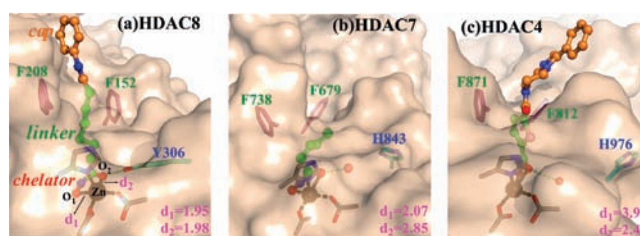

Figure 1. Active site of the enzyme−inhibitor complex in HDAC8 (a), HDAC7 (b), and HDAC4 (c). For HDAC8, the inhibitor is SAHA; for HDAC7, it is a truncated SAHA in the crystal structure; and for HDAC4, it is a SAHA-like hydroxamic acid. The two conserved phenylalanines are located at the entrance of the pocket. Y306 forms a hydrogen bond with SAHA in HDAC8 but is replaced by a His in HDAC7/4, in which a crystal water is close enough to form the hydrogen bond with the inhibitor. The oxygen−zinc distances d_1 and d_2 were measured from X-ray diffraction structures.[16,19,20]

hydroxamate inhibitors have been obtained, including HDAC8, a class-I enzyme,[15−18] and HDAC4 and HDAC7, two class-IIa enzymes.[19,20] As shown in Figures 1 and S1, despite all three isoforms having almost the same first zinc coordination shell, different hydroxamate−zinc coordination modes are observed: bidentate in HDAC8 (PDB ID 1T69[16]), monodentate in HDAC7 (PDB ID 3C0Z[20]), and weakly dentate with zinc in HDAC4 (PDB ID 2VQM[19]). A key distinction between class-I and class-IIa HDACs is that a tyrosine residue (Y306 in HDAC8) in the active site, which is conserved in all class-I HDACs, is replaced by a histidine in class-IIa enzymes. Experimental studies of HDAC4 and HDAC7 have shown that mutation of this histidine to tyrosine would significantly increase enzyme activity as well as its binding to hydroxamate LAQ-824.[9,19−21] Meanwhile, DFT calculations of zinc complexes have suggested that hydroxamic acid should be deprotonated upon its binding to the zinc ion, resulting in the tight bidentate complexation.[22] A current hypothesis is that the zinc−hydroxamate chelation mode in HDACs is determined by the protonation state of the hydroxamic acid: it is deprotonated in HDAC8 due to the existence of Y306, leading to the bidentate chelation.[9,22] Another distinction between class-I and class-IIa HDACs is the different orientations of the two conserved phenylalanines around the entrance of the binding pocket: bound to the linker component of SAHA with a “sandwich-like” configuration in HDAC8, but not in HDAC7 and HDAC4 (Figures 1 and S1). Experimental

Received: December 9, 2010
Published: April 01, 2011

 © 2011 American Chemical Society

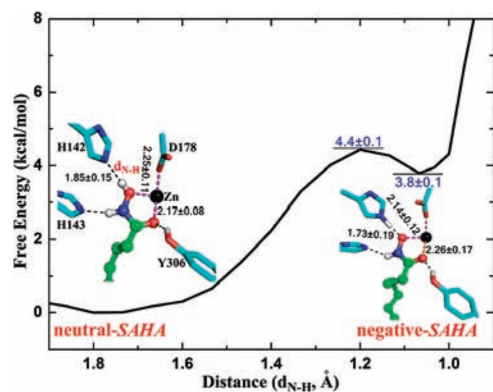

Figure 2. Free energy profile for the proton transfer from SAHA to His142. The distance between H142:N and SAHA:H (d_{N-H}) was chosen as the reaction coordinate. The statistical error is estimated by averaging the free energy difference between 5−15 ps and 15−25 ps.

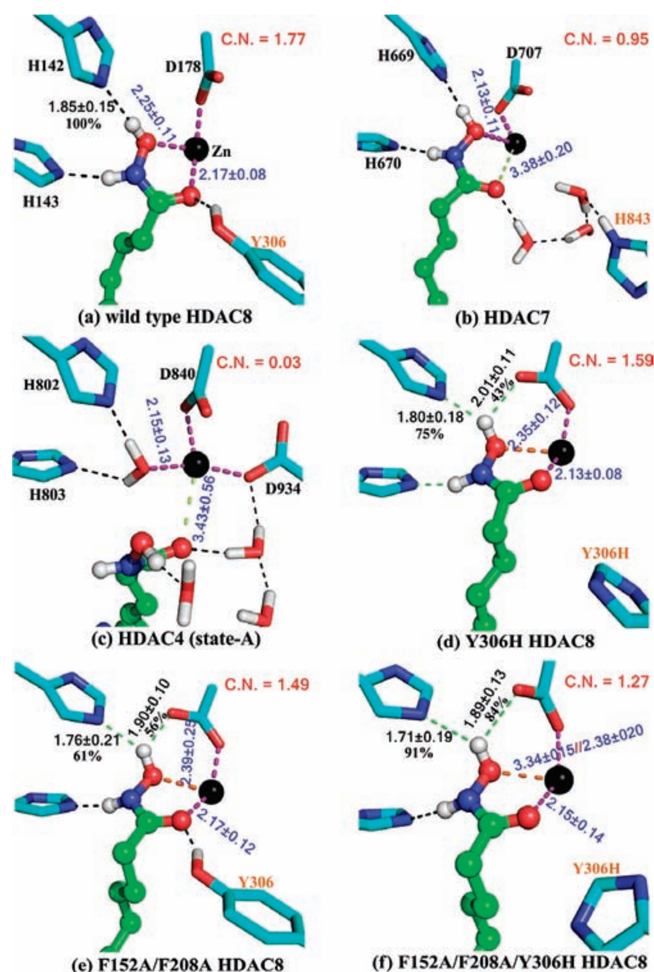

Figure 3. Illustration of zinc chelation modes and the hydrogen bond network for each model from our QM/MM MD simulations. C.N. means the coordination number between zinc and hydroxamate. C.N. = 1 if Zn−N ≤ 2.15 Å, 0 if Zn−N ≥ 2.40 Å, and is a linear scalar between 0 and 1 if Zn−N is between 2.15 and 2.40 Å. Similarly, the values of 2.20 and 2.60 Å are used for Zn−O, respectively. These values are chosen on the basis of a very recent analysis of the zinc enzyme structures database.[39]

studies found that mutation of these two Phe residues in HDAC1 led to an inactive enzyme.[23] Thus, it is intriguing to ask whether and how this distinct structural feature in the linker channel would affect the binding of HDAC inhibitors.

To elucidate the origin of the observed distinct zinc−hydroxamate chelation mode between class-I and class-IIa HDACs, we employed Born−Oppenheimer ab initio quantum mechanics/molecular mechanics molecular dynamics (QM/MM MD),[24−30] a state-of-the-art approach to simulating metallo-enzymes. It provides a first-principles description of interactions and dynamics of the zinc active site while explicitly taking into account the heterogeneous and fluctuating enzyme environment. The QM subsystem, including the zinc ion, the inhibitor, residues in the first coordination shell, and two histidines in the active site, was treated by the B3LYP functional with the Stuttgart ECP/basis set (SDD[31]) for the zinc atom and the 6-31G* basis set for all other atoms. This level of QM treatment[28,30,32−35] has been extensively tested and employed successfully to describe the zinc coordination shell. The QM/MM boundaries were described by the pseudobond approach with the improved parameters.[36] For each prepared enzyme system as well as umbrella sampling at each window along the reaction coordinate, 25 ps B3LYP(SDD,6-31G*) QM/MM MD simulations at 300 K were carried out with modified Q-Chem[37] and Tinker[38] programs.

Our first task was to examine whether the hydroxamic acid is deprotonated by His142 upon binding to HDAC8, leading to its bidendate chelation mode.[22] We employed ab initio QM/MM MD simulations with umbrella sampling to directly compute the free energy profile of this proton-transfer process to determine the free energy difference between these two states (Figure 2). We can see that the deprotonated-SAHA state, in which the proton is transferred to His142, is about 3.8 kcal/mol less stable than the neutral-SAHA state. This indicates that the hydroxamic acid, which is neutral in the aqueous environment, remains to be protonated upon binding to HDAC8, despite the existence of Y306. Moreover, we found that the zinc−hydroxamate chelation mode in HDAC8 is not dependent on the protonation state of SAHA, which is bidendate in both states (Figure 2).

We then carried out ab initio QM/MM MD simulations of HDAC7 and HDAC4, class-IIa enzymes, with a computational protocol similar to that employed for HDAC8.[28] The resulting hydroxamate chelation modes for all three HDACs are illustrated in Figure 3, and the distributions of the distances from the oxygen atoms (O_1 and O_2) of hydroxamate to the zinc atom are summarized in Figure S2. Our QM/MM MD simulations reproduce the coordination configurations in the crystal structures of wild-type HDAC8 and HDAC7 very well (Figure S1). Considering that the distance between O_2 and Zn in HDAC4 from our simulation (state A, 3.43 ± 0.56 Å) was longer than that in the crystal structure (2.49 Å), we set up another QM/MM MD simulation on HDAC4 (state B, Figure S3), in which the Zn−O_2 distance was restrained at 2.49 Å during the first 3 ps of QM/MM MD simulation, followed by another ∼20 ps of simulation without any restraints. The resulting trajectory shows that the originally bound water leaves the first zinc coordination shell and the hydroxamate is monodentate with Zn^{2+}. Nevertheless, both simulations indicate a four-fold zinc coordination shell in the HDAC4 complex. The widespread distribution of Zn−O distances indicates a loose binding of hydroxamate in HDAC4 (Figure S2).

So far, our simulations of wild-type HDACs confirm the experimental structural finding that, despite having the same coordinating ligands, different HDACs can have distinct zinc−hydroxamate chelation modes. To find the origin of such differences, we carried out further ab initio QM/MM MD simulations on three SAHA-HDAC8 mutants, i.e., single mutant Y306H,

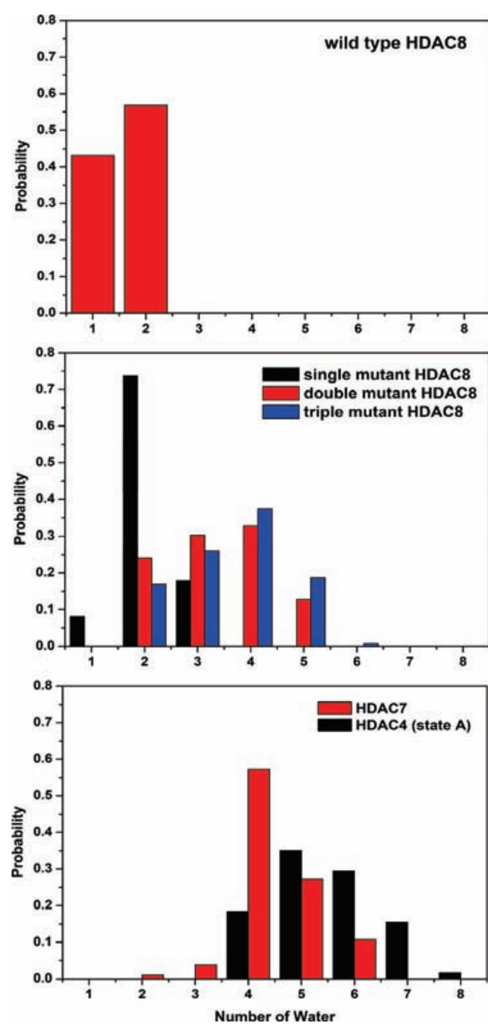

Figure 4. Number of water molecules in the binding pocket of each model during the last 20 ps QM/MM MD trajectory.

double mutant F152A/F208A, and triple mutant F152A/F208A/Y306H. The results in Figure 3 indicate that, although these mutations have little effect on the coordination interactions between zinc and amino acid residues, they do lead to significantly different zinc−hydroxamate chelation modes, especially for the triple mutant F152A/F208A/Y306H. For Y306H single mutant, the average coordination distance between SAHA-O_1 and zinc is elongated by 0.1 Å and its zinc-hydroxamate coordination number is reduced by about 0.2. For F152A/F208A double mutant, not only is the average coordination distance longer, but also the fluctuation is significantly larger, which indicates a more flexible and weaker zinc−hydroxamate coordination. For the triple mutant, the average value and the fluctuation of the coordination distance between SAHA-O_1 and zinc are significantly increased, and its distribution curve in Figure S2 clearly displays two distinct peaks, indicating that the SAHA chelation becomes monodentate to some extent. Thus, our simulations confirm that the existence of the active site tyrosine residue would strengthen the zinc−hydroxamate binding, consistent with experimental mutation results.[9,19−21] However, our results indicate that this residue alone would not determine the chelation mode of the hydroxamate.

By further analyzing all QM/MM MD simulations of HDACs, we find that the more water molecules inside the binding pocket,

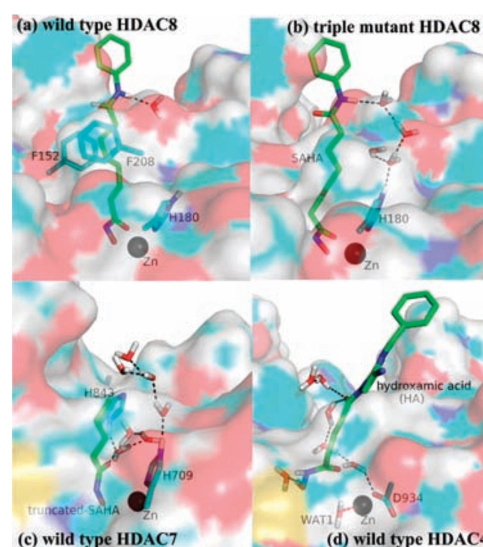

Figure 5. Comparison of the binding pockets in different models. A stable hydrogen-bonded water chain was observed during the QM/MM MD simulation with models b−d.

which mostly stay in the linker binding channel, the more likely the monodentate zinc−hydroxamate binding. From Figure 4, we can see that there are only one or two waters in the binding pocket of the wild-type HDAC8 and two in Y306H HDAC8, but on average four in F152A/F208A and Y306H/F152A/F208A HDAC8. For HDAC7 and HDAC4 models, there can be up to six water molecules. We can also see that in double/triple mutant HDAC8, wild-type HDAC7, or HDAC4, there exists at least one stable hydrogen-bonded water chain in the linker channel along which the waters enter into the zinc active site, as shown in Figures 5, S4, and S5. With the presence of more water molecules in the binding pocket, the dielectric constant would be increased, which in turn would lead to weaker electrostatic interactions between zinc and ligands in the binding site. Considering that Zn^{2+} has a saturated electronic configuration of d^{10}, its coordination with ligands is dominated by electrostatic interactions and thus would be weakened by the presence of more water molecules. Meanwhile, due to the presence of two carboxyl groups in the first coordination shell of HDACs, the flexibility of its zinc coordination has been previously found to be quite different from that in other zinc enzymes,[40] and it comes mostly from its chelation with the non-amino-acid ligand.[28] These would explain why different water molecules in the active site of HDACs would affect the binding mode of the hydroxamate despite having the same first coordination shell. Furthermore, Figure S6 indicates that the calculated electrostatic potential fitting charge on the zinc ion is reduced when more water molecules are in the binding pocket, leading to even weaker zinc−ligand interactions.

Different numbers of water molecules inside the binding pocket observed in distinct HDACs can be ascribed to the gating effect of two Phe residues around the pocket entrance. For HDAC7 and HDAC4, since the aromatic rings of both phenylalanines are away from the inhibitor and pointing toward the protein surface, the channel is wide enough to allow more water molecules to enter the pocket and form stable hydrogen bonds with the inhibitor and Zn-bound ligands. However, for wild-type HDAC8, F152/F208 and the linker constitute a "sandwich-like" conformation to block the channel and prevent water from entering the binding pocket. Volume calculations indicate that the binding pocket is 2225 ±

184 Å^3 in the wild-type HDAC8 (Figure S7), much smaller than those in HDAC7 and HDAC4 (4137 ± 206 and 4360 ± 262 Å^3, respectively). But the channel in HDAC8 (11.6 ± 1.3 Å) is deeper than those in HDAC7 (7.3 ± 0.6 Å) and HDAC4 (6.4 ± 1.0 Å), indicating that the channel in wild-type HDAC8 is much narrower. Even though the Y306H mutation of HDAC8 enlarges the vacant space of the pocket, the channel is still blocked by the conserved F152/F208 and the linker part of SAHA. Only after the F152A/F208A mutation is the channel blockage cleared, and extra room is available to allow more water molecules to enter the pocket. For the HDAC8 triple mutant F152A/F208A/Y306H (Figure S5), its entrance becomes significantly wider than that of the wild-type, the space is enlarged (3718 ± 223 Å^3), and the channel becomes less deep (10.1 ± 0.8 Å), which yields a binding pocket resembling those of HDAC7 and HDAC4. These results demonstrate the important gating effect of F152/F208 in HDAC8 and provide further support for our new mechanistic suggestion that the zinc—hydroxamate coordination mode in HDACs is modulated by water access to the linker binding channel.

In summary, our ab initio QM/MM MD simulations do not support the mechanistic hypothesis that the distinct zinc—hydroxamate chelation modes between two HDAC subclasses come from different protonation states of the hydroxamic acid. Instead, our simulation results suggest one novel mechanism regarding the interplay between the linker binding and the zinc chelation: the zinc—hydroxamate coordination mode in HDACs can be modulated by water access to the linker binding channel. This implies that, for the development of new class-IIa specific inhibitors, one intriguing direction to explore would be the design of a linker component to block the access of water molecules into the binding pocket.

■ ASSOCIATED CONTENT

S Supporting Information. Computational details; Figures S1—S7; complete refs 16 and 37. This material is available free of charge via the Internet at http://pubs.acs.org.

■ AUTHOR INFORMATION

Corresponding Author

zxcao@xmu.edu.cn; yingkai.zhang@nyu.edu

■ ACKNOWLEDGMENT

This work was supported by Chinese NSF (20733002 and 20873105) and the Ministry of Science and Technology (2011CB808504) and American NIH (R01-GM079223) and NSF (CHE-CAREER-0448156, TeraGrid resources). We thank NYU-ITS for providing computational resources and Dr. Shenglong Wang for computing support.

■ REFERENCES

(1) Kouzarides, T. *Cell* **2007**, *128*, 693–705.
(2) Cole, P. A. *Nat. Chem. Biol.* **2008**, *4*, 590–597.
(3) Smith, B. C.; Denu, J. M. *BBA-Gene Regul. Mech.* **2009**, *1789*, 45–57.
(4) Haberland, M.; Montgomery, R. L.; Olson, E. N. *Nat. Rev. Genet.* **2009**, *10*, 32–42.
(5) Kazantsev, A. G.; Thompson, L. M. *Nat. Rev. Drug Discov.* **2008**, *7*, 854–868.
(6) Paris, M.; Porcelloni, M.; Binaschi, M.; Fattori, D. *J. Med. Chem.* **2008**, *51*, 1505–1529.
(7) Bolden, J. E.; Peart, M. J.; Johnstone, R. W. *Nat. Rev. Drug Discov.* **2006**, *5*, 769–784.
(8) Minucci, S.; Pelicci, P. G. *Nat. Rev. Cancer* **2006**, *6*, 38–51.
(9) Bradner, J. E.; West, N.; Grachan, M. L.; Greenberg, E. F.; Haggarty, S. J.; Warnow, T.; Mazitschek, R. *Nat. Chem. Biol.* **2010**, *6*, 238–243.
(10) Bertrand, P. *Eur. J. Med. Chem.* **2010**, *45*, 2095–2116.
(11) Bieliauskas, A. V.; Pflum, M. K. H. *Chem. Soc. Rev.* **2008**, *37*, 1402–1413.
(12) Estiu, G.; Greenberg, E.; Harrison, C. B.; Kwiatkowski, N. P.; Mazitschek, R.; Bradner, J. E.; Wiest, O. *J. Med. Chem.* **2008**, *51*, 2898–2906.
(13) Olsen, C. A.; Ghadiri, M. R. *J. Med. Chem.* **2009**, *52*, 7836–46.
(14) Sternson, S. M.; Wong, J. C.; Grozinger, C. M.; Schreiber, S. L. *Org. Lett.* **2001**, *3*, 4239–4242.
(15) Vannini, A.; Volpari, C.; Filocamo, G.; Casavola, E. C.; Brunetti, M.; Renzoni, D.; Chakravarty, P.; Paolini, C.; De Francesco, R.; Gallinari, P.; Steinkuhler, C.; Di Marco, S. *Proc. Natl. Acad. Sci. U.S.A.* **2004**, *101*, 15064–15069.
(16) Somoza, J. R.; et al. *Structure* **2004**, *12*, 1325–1334.
(17) Vannini, A.; Volpari, C.; Gallinari, P.; Jones, P.; Mattu, M.; Carfi, A.; De Francesco, R.; Steinkuhler, C.; Di Marco, S. *Embo Rep.* **2007**, *8*, 879–884.
(18) Dowling, D. P.; Gantt, S. L.; Gattis, S. G.; Fierke, C. A.; Christianson, D. W. *Biochemistry* **2008**, *47*, 13554–13563.
(19) Bottomley, M. J.; Lo Surdo, P.; Di Giovine, P.; Cirillo, A.; Scarpelli, R.; Ferrigno, F.; Jones, P.; Neddermann, P.; De Francesco, R.; Steinkuhler, C.; Gallinari, P.; Carfi, A. *J. Biol. Chem.* **2008**, *283*, 26694–26704.
(20) Schuetz, A.; Min, J.; Allali-Hassani, A.; Schapira, M.; Shuen, M.; Loppnau, P.; Mazitschek, R.; Kwiatkowski, N. P.; Lewis, T. A.; Maglathin, R. L.; McLean, T. H.; Bochkarev, A.; Plotnikov, A. N.; Vedadi, M.; Arrowsmith, C. H. *J. Biol. Chem.* **2008**, *283*, 11355–11363.
(21) Lahm, A.; Paolini, C.; Pallaoro, M.; Nardi, M. C.; Jones, P.; Neddermann, P.; Sambucini, S.; Bottomley, M. J.; Lo Surdo, P.; Carfi, A.; Koch, U.; De Francesco, R.; Steinkuhler, C.; Gallinari, P. *Proc. Natl. Acad. Sci. U.S.A.* **2007**, *104*, 17335–17340.
(22) Wang, D. F.; Helquist, P.; Wiest, O. *J. Org. Chem.* **2007**, *72*, 5446–5449.
(23) Weerasinghe, S. V. W.; Estiu, G.; Wiest, O.; Pflum, M. K. H. *J. Med. Chem.* **2008**, *51*, 5542–5551.
(24) Hu, P.; Wang, S.; Zhang, Y. *J. Am. Chem. Soc.* **2008**, *130*, 3806–3813.
(25) Hu, P.; Wang, S. L.; Zhang, Y. K. *J. Am. Chem. Soc.* **2008**, *130*, 16721–16728.
(26) Ke, Z. H.; Zhou, Y. Z.; Hu, P.; Wang, S. L.; Xie, D. Q.; Zhang, Y. K. *J. Phys. Chem. B* **2009**, *113*, 12750–12758.
(27) Wang, S. L.; Hu, P.; Zhang, Y. K. *J. Phys. Chem. B* **2007**, *111*, 3758–3764.
(28) Wu, R.; Hu, P.; Wang, S.; Cao, Z.; Zhang, Y. *J. Chem. Theory Comput.* **2010**, *6*, 337–343.
(29) Zhou, Y. Z.; Wang, S. L.; Zhang, Y. K. *J. Phys. Chem. B* **2010**, *114*, 8817–8825.
(30) Wu, R. B.; Wang, S. L.; Zhou, N. J.; Cao, Z. X.; Zhang, Y. K. *J. Am. Chem. Soc.* **2010**, *132*, 9471.
(31) Dolg, M.; Wedig, U.; Stoll, H.; Preuss, H. *J. Chem. Phys.* **1987**, *86*, 866–872.
(32) Sousa, S. F.; Fernandes, P. A.; Ramos, M. J. *Biophys. J.* **2005**, *88*, 483–494.
(33) Sousa, S. F.; Fernandes, P. A.; Ramos, M. J. *J. Am. Chem. Soc.* **2007**, *129*, 1378–1385.
(34) Xiao, C. Y.; Zhang, Y. K. *J. Phys. Chem. B* **2007**, *111*, 6229–6235.
(35) Corminboeuf, C.; Hu, P.; Tuckerman, M. E.; Zhang, Y. K. *J. Am. Chem. Soc.* **2006**, *128*, 4530–4531.
(36) Zhang, Y. K. *J. Chem. Phys.* **2005**, *122*, 024114.
(37) Shao, Y.; et al. *Q-Chem*, version 3.0; Pittsburgh, PA, 2006.
(38) Ponder, J. W. *TINKER, Software Tools for Molecular Design*, version 4.2; 2004.
(39) Tamames, B.; Sousa, S. F.; Tamames, J.; Fernandes, P. A.; Ramos, M. J. *Proteins: Struct., Funct., Bioinf.* **2007**, *69*, 466–475.
(40) Papoian, G. A.; DeGrado, W. F.; Klein, M. L. *J. Am. Chem. Soc.* **2003**, *125*, 560–569.